Cellular Immunology 344 (2019) 103948

Contents lists available at ScienceDirect

Cellular Immunology

journal homepage: www.elsevier.com/locate/ycimm

Research paper

High iodine induces DNA damage in autoimmune thyroiditis partially by inhibiting the DNA repair protein MTH1

Fuqiang Li*, Yijun Wu, Liang Chen, Liang Hu, Feng Zhu, Qiwen He

Thyroid Disease Diagnosis and Treatment Center, The First Affiliated Hospital, School of Medicine, Zhejiang University, Hangzhou 310003, China

ARTICLE INFO

Keywords:
Iodine
DNA damage
Apoptosis
Inflammation
MTH1

ABSTRACT

This study aims to investigate the level of DNA damage in high iodine (HI)-induced autoimmune thyroiditis (AIT), and to explore the role of DNA repair protein MutT homolog-1 (MTH1) in this process. The levels of pro-inflammatory cytokines tumor necrosis factor (TNF)-α, interleukin (IL)-6, and IL-8 were measured using qRT-PCR and ELISA. The apoptosis was evaluated using TUNEL staining. The pathological changes of thyroid tissues were evaluated using hematoxylin and eosin (HE) staining. The DNA damage was assessed by determining the expression of 8-hydroxy-2′deoxyguanosine (8-OHdG; an indicator of oxidative DNA damage) and performing the Comet assay. Our results showed that both the HI-treated NOD.H-2^{h4} mice (experimental AIT mice) and the HI-treated mouse thyroid follicular epithelial cells showed enhanced inflammation, apoptosis, and DNA damage level, accompanied by decreased MTH1 expression. Importantly, overexpression of MTH1 effectively abrogated the HI-induced enhancement of inflammation, apoptosis, and DNA damage in mouse thyroid follicular epithelial cells. In conclusion, HI treatment induces DNA damage in AIT, at least in part, by inhibiting the DNA repair protein MTH1.

1. Introduction

Autoimmune thyroiditis (AIT) is considered as one of the most common autoimmune diseases. Hashimoto's thyroiditis (HT) is a major type of AIT and pathologically characterized by lymphocyte infiltration of the thyroid gland and thyroid follicular tissue lesions [1,2]. Indeed, HT is the most common cause of hypothyroidism in developed countries. It has been currently accepted that genetic susceptibility, environmental factors, and immune disorders contribute to the development of HT [3,4]. Up to date, there remains no effective preventative or therapeutic treatment for AIT. Therefore, elucidation of the pathogenesis of AIT is important for improving the prevention and treatment for AIT.

Increasing studies have shown that chronic intake of high-iodine (HI) is positively associated with the increased incidence of AIT [5–8]. Chronic exposure to HI intake may induce AIT in susceptible individuals [7,9]. Mechanistically, chronic HI intake triggers AIT, partly because highly iodinated thyroglobulin is more immunogenic [3]. Studies also show that in susceptible individuals, iodine excess increases intra-thyroid infiltrating Th17 cells and inhibits T regulatory cells development, while it triggers an abnormal expression of tumor necrosis factor-related apoptosis-inducing ligand (TRAIL) in thyrocytes, thus inducing thyrocyte apoptosis and parenchymal destruction [5,8]. Although the above-mentioned mechanisms can partially explain the HI-induced AIT, there is little literature linking DNA damage and the HI-induced AIT.

In this study, we aimed to investigate the level of DNA damage upon HI treatment in AIT, and to explore the role of DNA repair protein MutT homolog-1 (MTH1) in this process. To address this, we used the HI-treated NOD.H-2^{h4} mice and the HI-treated mouse thyroid follicular epithelial cells as a mouse and cellular AIT model, respectively.

2. Materials and methods

2.1. Esthical approval

This study was approved by the Ethics Committee of The First Affiliated Hospital, School of Medicine, Zhejiang University (Approval number: 2019–774). The experiments were carried out according to the guidelines laid down by the institution's animal welfare committee, and conform to the principles and regulations, as described in the Editorial by Grundy (2015).

2.2. Animals

NOD.H-2^{h4} mice is an important animal model of autoimmune

* Corresponding author at: No. 79 Qingchun Road, Hangzhou 310003, China.
E-mail address: cd20070410@zju.edu.cn (F. Li).

https://doi.org/10.1016/j.cellimm.2019.103948
Received 26 March 2019; Received in revised form 11 June 2019; Accepted 1 July 2019
Available online 02 July 2019
0008-8749/

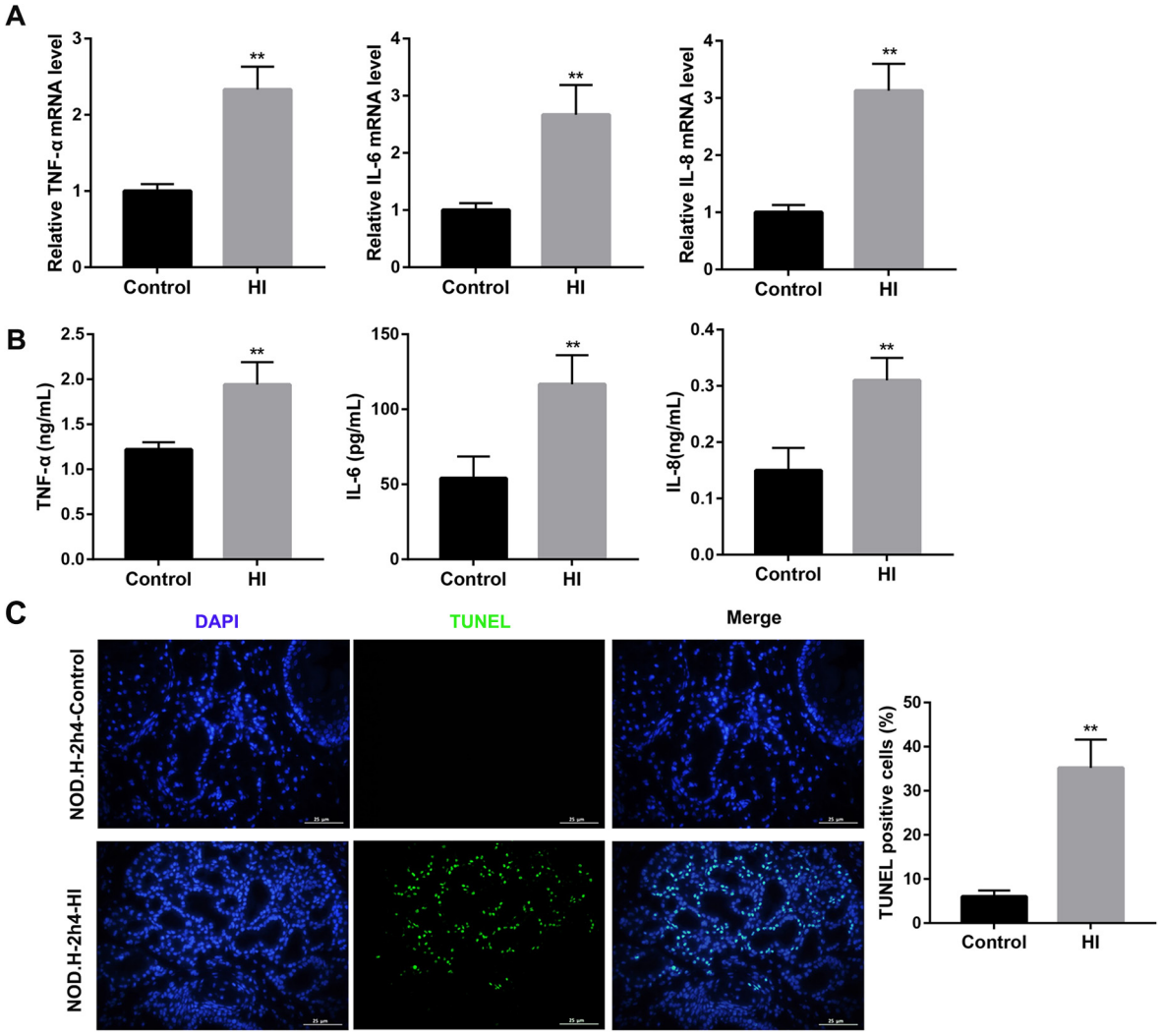

Fig. 1. Enhanced inflammation and apoptosis in HI-treated mice. NOD.H-2^{h4} mice were randomly divided into two groups: control and HI group (n = 10/group). (A) The mRNA levels of pro-inflammatory cytokines TNF-α, IL-6, and IL-8 in sera were measured using qRT-PCR. (B) The serum levels of pro-inflammatory cytokines TNF-α, IL-6, and IL-8 were measured using ELISA. (C) TUNEL staining was performed to observe the level of apoptosis in thyroid tissues. Scale bar: 25 μm. Notes: The apoptotic cells are shown as green fluorescence with fluorescein isothiocyanate staining. The nucleus was stained with DAPI. The number of TUNEL-positive cells (green) was compared with the total cells using Image-Pro Plus 6.0 software and expressed as a percentage. HI, high iodine; TNF-α, tumor necrosis factor-α; IL-6, interleukin-6; IL-8, interleukin-8; TUNEL, TdT-mediated dUTP nick-end labeling.

thyroiditis [10]. All the NOD.H-2^{h4} mice (4-week old, female) were raised under a specific pathogen-free environment in a 12 h light/12 h dark cycle throughout the experimental period. All experimental procedures were performed in strict accordance with the guidelines for the Care and Use of Laboratory Animals of the National Institutes of Health.

The mice were randomly divided into two groups (n = 10/group): control and high iodine (HI) group. The mice in the HI group were fed with sterile water containing 0.05% sodium iodide (NaI; 500 mg/L, with iodine intake of approximately 2000 μg/d for each mouse), and the mice in the control group were fed with sterile water. At the 12th week after the start of the experiment, the animals in each group were anesthetized with ketamine and xylazine, and then sacrificed by dislocation of the cervical vertebra. The thyroid tissues were isolated and fixed in 4% paraformaldehyde and then embedded in paraffin before being cut into 5-μm thick sections for further use.

2.3. Isolation and culture of mouse thyroid follicular epithelial cells

The thyroid tissues were exercised from 6 to 8 week-old BALB/c mice and digested with collagenase I/neutral protease to obtain the thyroid follicular epithelial cells. Briefly, the BALB/c mice were sacrificed by dislocation of the cervical vertebra and the thyroid tissues were then exercised under sterile conditions. The thyroid tissues of each leaf were cut into small pieces of about 1.5 mm^3 and transferred to 1.5 mL Eppendorf tubes. After washed in serum-free medium for two times, the tissues were digested using 1 mL digestive solution containing 10^3 KU/L collagenase I (Gibco) and 1.35 kU/L dispase (Gibco) for 40 min at 37 °C in water. After centrifugation at 800 r/min for 10 min, the supernatant containing the digestive enzyme was discarded, and the precipitation was suspended in the F-12 complete medium (Sigma) containing fetal calf serum (FCS, 10%, Hyclone), thyrotropin (l U/L), hydrocortisone (5 mg/L), transferrin (5 mg/L), insulin (10 mg/L), L-Glutamine (0.3 g/L), penicillin (10^5 U/L) and streptomycin (100 mg/L). The cells were then seeded on a 24-well plate and maintained in humidified air with 5% CO_2 at 37 °C. Media was changed the next day and the FCS concentration was reduced to 5%. After that, the media was changed every three days.

2.4. Plasmid construction and transfection

To overexpress MTH1, the full-length MTH1 cDNA fragments were cloned into the pcDNA 3.1 plasmid (Invitrogen; Thermo Fisher

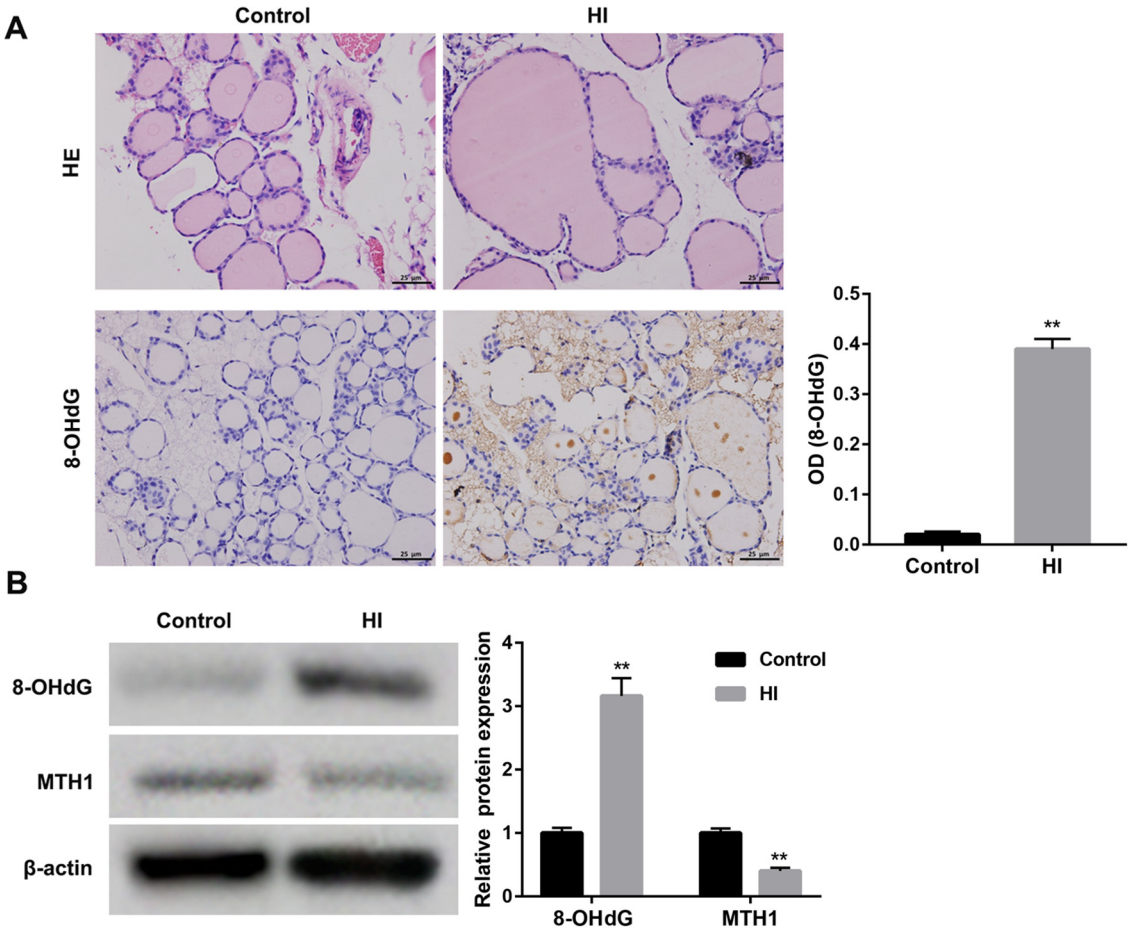

Fig. 2. Enhanced inflammation and DNA damage in HI-treated mice. (A) HE staining of thyroid tissues was performed to examine the pathological changes in thyroid tissues. The immunohistochemical staining for 8-OHdG was performed to observe the level of DNA damage in thyroid tissues. Scale bar: 25 μm. Positive 8-OHdG staining (brown) was observed and assessed using Image-Pro Plus 6.0 software to obtain the average optical density (OD) value of the selected field (×400). (B) Western blot was performed to detect the protein levels of 8-OHdG and DNA repair protein MTH1 in thyroid tissues. β-actin served as a loading control. $^{**}p < 0.01$ *vs.* the control group. HI, high iodine; HE, hematoxylin and eosin; 8-OHdG, 8-hydroxy-2′deoxyguanosine; MTH1, MutT homolog-1.

Scientific, Inc.), generating pcDNA3.1-MTH1 plasmids (MTH1-OE). The orientation and sequence of the recombinant plasmid were confirmed by restriction enzyme digestion and DNA sequencing. An empty pcDNA3.1 vector was used as a negative control (OE-NC). The thyroid follicular epithelial cells were transfected with these constructs using Lipofectamine™ 3000 (Invitrogen; Thermo Fisher Scientific, Inc.) according to the manufacturer's instructions.

2.5. Enzyme-linked immunosorbent assay (ELISA)

The levels of pro-inflammatory cytokines tumor necrosis factor (TNF)-α, interleukin (IL)-6, and IL-8 in mouse serum or cell supernatant of the thyroid follicular epithelial cells were measured using their commercial ELISA kits (R&D Systems, USA) according to the manufacturers' protocols.

2.6. TdT-mediated dUTP nick-end labeling (TUNEL) staining

TUNEL staining was performed to observe the apoptosis in thyroid tissues. Briefly, the 5-μm thick sections were incubated with the TUNEL kit (Thermo Fisher Scientific, Waltham, MA, USA) according to the manufacturer's instructions. Finally, the sections were sealed and images were visualized under an inverted fluorescence microscope (Olympus Corporation, Tokyo, Japan). The apoptotic cells are shown as green fluorescence with fluorescein isothiocyanate staining. The nucleus was stained with DAPI. The cell apoptosis in the thyroid follicular epithelial cells was assessed by One Step TUNEL Apoptosis Assay Kit (Beyotime, Shanghai, China) according to the manufacturer's instructions. The number of TUNEL-positive cells (green) was counted in 10 randomly selected fields. The number of TUNEL-positive cells was compared with the total cells using Image-Pro Plus 6.0 software and expressed as a percentage.

2.7. Hematoxylin and eosin (HE) staining

HE staining was performed to examine the pathological changes of thyroid tissues. Briefly, the 5-μm thick sections were stained using HE following a routine staining procedure and examined under an Olympus BH-2 light microscope (×400; Olympus, Tokyo, Japan).

2.8. Immunohistochemical staining for 8-hydroxy-2′deoxyguanosine (8-OHdG)

The immunohistochemical staining for 8-OHdG was performed to observe the level of DNA damage. Briefly, the 5-μm thick sections were dewaxed, rehydrated, and then incubated with 3% H_2O_2 for 20 min at room temperature. After that, the sections were washed with PBS three times and treated with trypsinization to retrieve the antigen. After being blocked with 5% normal goat serum for 30 min, the sections were incubated with a primary antibody against 8-OHdG (Santa Cruz Biotechnology, Dallas, TX, USA) at 4 °C overnight. After that, the sections were washed with PBS three times and then incubated with

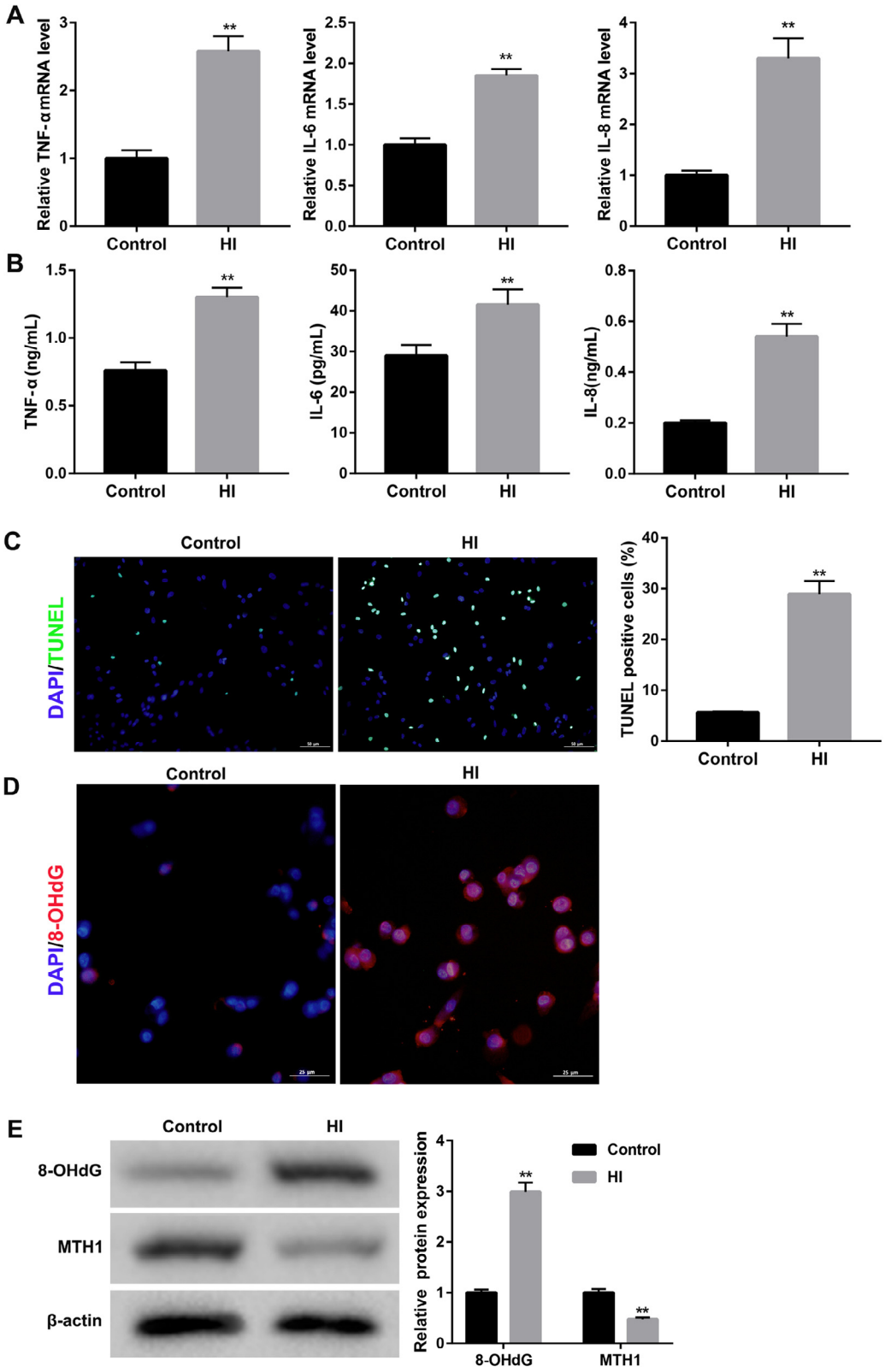

Fig. 3. Enhanced inflammation, apoptosis, and DNA damage in HI-treated mouse thyroid follicular epithelial cells. The primary mouse thyroid follicular epithelial cells were randomly divided into two groups: the control group and HI treatment group (10 mg/L NaI, 48 h). (A) The mRNA levels of pro-inflammatory cytokines TNF-α, IL-6, and IL-8 in the cells were measured using qRT-PCR. (B) The levels of pro-inflammatory cytokines TNF-α, IL-6, and IL-8 in the cell supernatant were measured using ELISA. (C) TUNEL staining was performed to observe cell apoptosis. Notes: The nick-ends were labeled in green indicating the apoptotic cells and the cell nuclei were stained with DAPI and appeared blue in color. Scale bar: 50 μm. The number of TUNEL-positive cells (green) was compared with the total cells using Image-Pro Plus 6.0 software and expressed as a percentage. (D) The immunofluorescence staining showing the localization of 8-OHdG labeled with AlexaFluor568, showing the oxidative lesion in red. Cell nuclei were labeled in blue by DAPI. Scale bar: 25 μm. (E) Western blot was performed to detect the protein levels of 8-OHdG and DNA repair protein MTH1. $^{**}p < 0.01$ *vs.* the control group. Data are presented as the mean ± SD (n = 3). HI, high iodine; TNF-α, tumor necrosis factor-α; IL-6, interleukin-6; IL-8, interleukin-8; TUNEL, TdT-mediated dUTP nick-end labeling; 8-OHdG, 8-hydroxy-2′deoxyguanosine; MTH1, MutT homolog-1; SD, standard deviation.

biotinylated secondary antibody for 25 min at room temperature, followed by incubation with horseradish peroxide (HRP)-conjugated streptavidin for 20 min at room temperature. Then sections were stained with diaminobenzidine (DAB), counterstained with hematoxylin, dehydrated, and then embedded in paraffin. The sections were analyzed using an Olympus BH-2 light microscope (Olympus).

2.9. Immunofluorescence staining for 8-OHdG

Immunofluorescence staining for 8-OHdG was performed as previously described, with some alterations [11]. Briefly, the thyroid follicular epithelial cells were fixed using 4% paraformaldehyde and washed three times with bi-distilled water. After permeabilization using 30 mL 0.3% Triton-X 100 in PBS at 4 °C for 5 min, slides were washed

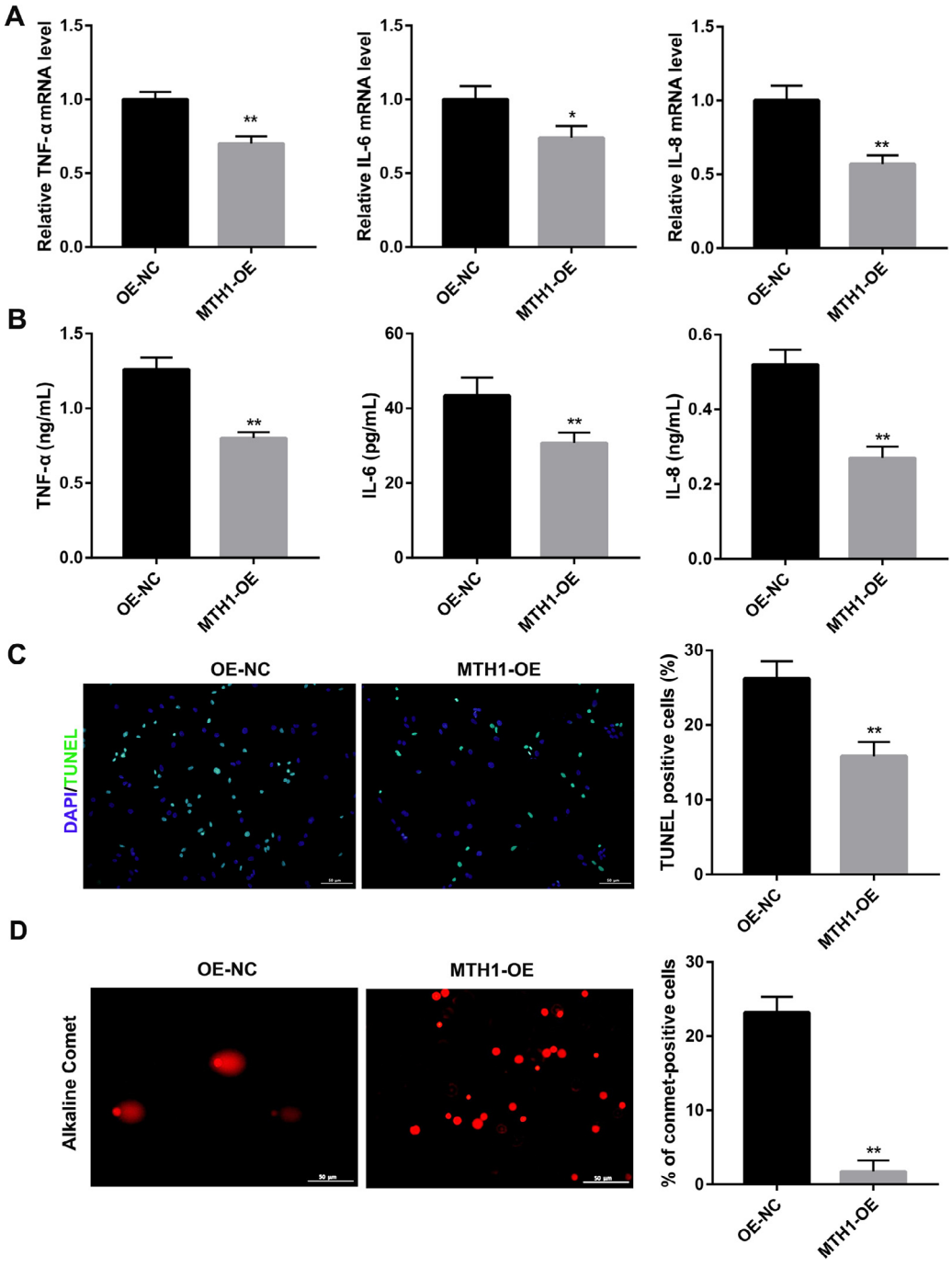

Fig. 4. MTH1 overexpression inhibited inflammation, apoptosis, and DNA damage in HI-treated mouse thyroid follicular epithelial cells. The thyroid follicular epithelial cells were transfected with pcDNA3.1-MTH1 to overexpress MTH1 (MTH1 OE), or empty pcDNA3.1 plasmid as a negative control (OE NC), followed by HI treatment (10 mg/L NaI, 48 h). (A) The mRNA levels of pro-inflammatory cytokines TNF-α, IL-6, and IL-8 in the cells were measured using qRT-PCR. (B) The levels of pro-inflammatory cytokines TNF-α, IL-6, and IL-8 in the cell supernatant were measured using ELISA. (C) TUNEL staining was performed to observe cell apoptosis. Notes: The nick-ends were labeled in green indicating the apoptotic cells and the cell nuclei were stained with DAPI and appeared blue in color. Scale bar: 50 μm. The number of TUNEL-positive cells (green) was compared with the total cells using Image-Pro Plus 6.0 software and expressed as a percentage. (D) Cellular DNA damage was determined using the Comet assay. Hundreds of cells were scored to calculate the overall percentage of comet tail-positive cells in 5 randomly selected fields (×200, scale bar: 50 μm). $^{**}p < 0.01$ *vs.* the OE NC group. Data are presented as the mean ± SD (n = 3). MTH1, MutT homolog-1; HI, high iodine; TNF-α, tumor necrosis factor-α; IL-6, interleukin-6; IL-8, interleukin-8; TUNEL, TdT-mediated dUTP nick-end labeling; 8-OHdG, 8-hydroxy-2′deoxyguanosine; MTH1, MutT homolog-1; SD, standard deviation.

twice with PBS. After being blocked with 10% goat serum, the slides were incubated with a mouse monoclonal antibody (1:1000, Abcam) at 4 °C overnight, followed by incubation with a goat anti-mouse secondary antibody labeled with fluorescent orange-red Alex Fluor 568 (Invitrogen, Camarillo, CA, USA) at 37 °C for 1 h. Subsequently, slides were washed three times with PBS and stained with DAPI. Finally, the sections were sealed and images were visualized under an inverted fluorescence microscope (Olympus Corporation, Tokyo, Japan).

2.10. Western blot

Total protein from tissues and cells was extracted using the radioimmunoprecipitation assay (RIPA) buffer (Beyotime). The protein concentrations were determined by BCA assay. Then equal protein from cell lysates was separated by 10% SDS-PAGE gels and electrotransferred onto PVDF membranes (Millipore Corp., Billerica, MA, USA). The membranes were blocked with 5% skim milk at room temperature for 2 h and then incubated overnight at 4 °C with the following primary antibodies against 8-OHdG (1:500; Abbiotec, San Diego, CA, USA), MTH1 (1:500; Santa Cruz Biotechnology Inc.), and β-actin (1:1000; Santa Cruz Biotechnology Inc.) overnight at 4 °C, followed by the HRP-conjugated secondary antibodies (1:2000; Santa Cruz Biotechnology Inc.) at room temperature for 2 h. The protein was detected using an enhanced chemiluminescence kit (Pierce; Thermo Fisher Scientific, Inc.) and the band intensity was quantified with Quantity One Software. β-actin served as a loading control.

2.11. Single-cell gel electrophoresis (Comet assay)

Cellular DNA damage, in terms of DNA strand breaks, was

determined using the Comet assay as previously described [12], with some modifications. Briefly, after treatment with high iodine, the transfected cells were harvested and resuspended in ice-cold PBS. Approximately 1×10^4 cells in a volume of 100 μL of 1.5% (w/v) low-melting-point agarose were pipetted onto a frosted glass slide coated with a thin layer of 1.0% (w/v) agarose, covered with a coverslip to spread it evenly, and allowed to set at 4 °C for 10 min. Following removal of the coverslip, the slides were immersed in ice-cold lysis buffer containing 2.5 mol/L NaCl, 10 mmol/L Tris, 100 mmol/L Na2-EDTA, and 1% (w/v) *N*-lauroylsarcosine, adjusted to pH10.0, and 1.0% Triton X-100 was added immediately before use. After 2 h at 4 °C, the slides were placed into a horizontal electrophoresis tank filled with buffer (0.3 mol/L NaOH, 1 mmol/L EDTA (pH13)) and subjected to electrophoresis for 20 min at 300 mA. Slides were transferred to neutralization buffer (0.2 mol/L Tris-HCl) for washes three times and stained with 50 μL of 2 μg/mL ethidium bromide for 5 min. Following a final wash in double-distilled water, the gels were covered with glass coverslips. The single cell electrophoresis images were observed under a fluorescence microscope (Olympus Corporation) and analyzed by CometScore software.

2.12. Statistical analysis

All statistical analyses were performed using SPSS 16.0 (SPSS, Inc., Chicago, IL, USA). The data are presented as the mean ± standard deviation (SD) from three independent experiments. The differences among three or more groups were analyzed using one-way analysis of variance (ANOVA). $p < 0.05$ was considered to indicate a statistically significant difference.

3. Results

3.1. Enhanced inflammation, apoptosis, and DNA damage in HI-treated mice

To investigate the effect of HI treatment on inflammation, apoptosis, and DNA damage *in vivo*, the NOD.H-2^{h4} mice were fed with sterile water containing 0.05% NaI (HI group) or sterile water (control group). The serum mRNA levels of pro-inflammatory cytokines TNF-α, IL-6, and IL-8 were significantly upregulated in the HI group compared with the control group (Fig. 1A). ELISA analysis further consolidated the qRT-PCR results (Fig. 1B). Furthermore, the percentage of TUNEL-positive cells was notably higher in the thyroid tissues of the HI group than that in the control group (Fig. 1C), indicating the apoptosis induction in the thyroid tissues by HI treatment. HE staining also showed enlarged follicular lumen in the mouse thyroid tissues from the HI model mice (Fig. 2A). Moreover, the immunohistochemical staining for 8-OHdG (an indicator of oxidative DNA damage) indicated an increase in the level of oxidative DNA damage in the HI-treated thyroid tissues compared with the control group (Fig. 2A). Additionally, western blot analysis showed that the protein level of 8-OHdG was significantly higher, whereas the protein level of the DNA repair protein MTH1 was significantly lower in the HI group compared with the control group (Fig. 2B). These results indicate that HI treatment induces inflammation, apoptosis, and DNA damage in HI-treated mice.

3.2. Enhanced inflammation, apoptosis, and DNA damage in HI-treated mouse thyroid follicular epithelial cells

To further investigate the effect of HI treatment on inflammation, DNA damage, and apoptosis *in vitro*, the mouse thyroid follicular epithelial cells were isolated from BALB/c mice and randomly divided into the control and HI group. Results of qRT-PCR and ELISA revealed that the levels of pro-inflammatory cytokines TNF-α, IL-6, and IL-8 in the cell supernatant were notably upregulated in the HI group compared with the control group (Fig. 3A and B). Furthermore, the percentage of TUNEL-positive cells was significantly higher in the HI group than that in the control group (Fig. 3C). Moreover, the immunofluorescence staining for 8-OHdG indicated an increase in the level of oxidative DNA damage in the HI-treated cells compared with the control group (Fig. 3D). Additionally, western blot analysis showed that the protein level of 8-OHdG was significantly higher, whereas the protein level of the DNA repair protein MTH1 was significantly lower in the HI group compared with the control group (Fig. 3E). These results indicate that HI treatment induces inflammation, apoptosis, and DNA damage in mouse thyroid follicular epithelial cells.

3.3. MTH1 overexpression inhibited inflammation, apoptosis, and DNA damage in HI-treated mouse thyroid follicular epithelial cells

Finally, we explored the effect of the DNA repair protein MTH1 on HI-induced inflammation, DNA damage, and apoptosis *in vitro*. MTH1 overexpression significantly downregulated the HI-induced levels of pro-inflammatory cytokines TNF-α, IL-6, and IL-8 in the cell supernatant (Fig. 4A and B). Furthermore, MTH1 overexpression notably decreased the HI-induced percentage of TUNEL-positive cells (Fig. 4C). Moreover, MTH1 overexpression effectively inhibited the HI-induced percentage of comet tail-positive cells, indicating the suppression of DNA damage by MTHI overexpression (Fig. 4D). Together, these results indicate that MTH1 overexpression significantly inhibits the HI-induced inflammation, apoptosis, and DNA damage in mouse thyroid follicular epithelial cells.

4. Discussion

The white race, female sex, older age, and increased consumption of iodine have been considered as risk factors for AIT [2]. Especially, increasing studies have provided evidence that in areas with excess iodine intake, increased incidence of AIT marked by high titers of thyroid peroxidase and thyroglobulin antibodies has occurred [5–9]. A recent study showed that serum levels of inflammatory cytokines TNF-α, IL-6, and IL-1β are significantly increased in the NOD.H-2^{h4} mice fed with water containing sodium iodide [13]. Studies also show that iodine excess induces thyrocyte apoptosis [5,8]. In line with these studies, the results in the present study showed enhanced inflammation and apoptosis in both the HI-treated mice and the HI-treated mouse thyroid follicular epithelial cells.

Existing evidence has unraveled the possible mechanisms of HI-induced AIT: 1) The direct toxic effect of HI on thyroid cells- HI produces excessive free radicals and damages cell biofilm and induces thyroid immune dysfunction; 2) Iodine intake enhances the immunogenicity of thyroglobulin with genetic susceptibility and promotes AIT development; 3) Iodine excess increases intra-thyroid infiltrating Th17 cells and inhibits T regulatory cells development, while it triggers an abnormal expression of TRAIL in thyrocytes, thus inducing thyrocyte apoptosis and parenchymal destruction [5,8]. In addition, a recent study suggested that excessive iodine consumption promoted DNA damage of lymphocytes and led to lymphocytic impairment that might be the potential cause of autoimmune thyroid diseases [14]. DNA damage constitutes a major threat to genetic integrity and has thus been recognized as important factors in contributing to inflammation and even carcinogenesis [15,16]. Here, we detected the levels of DNA damage in thyroid cells under HI conditions and found that HI treatment also triggered DNA damage when inducing inflammation and apoptosis.

8-OHdG is an oxidation product most frequently measured as an important indicator of oxidative DNA damage [17]. The results in the present study showed that HI treatment increased levels of 8-OHdG, whereas decreased levels of MTH1 in both the HI-treated mice and the HI-treated mouse thyroid follicular epithelial cells. MTH1 is an oxidative DNA damage repair enzyme that is mainly responsible for the “clean-up” of oxidized deoxynucleoside triphosphates (dNTPs) in nucleotide pools to prevent the incorporation of damaged bases during

DNA replication [18,19]. Accordingly, these data indicate that HI treatment increases the level of oxidative DNA damage in both the HI-treated mice and the HI-treated mouse thyroid follicular epithelial cells. Furthermore, the results in this study also showed that HI treatment induced comet-like tail in mouse thyroid follicular epithelial cells. Comet assay is a simple method for measuring DNA strand breaks in eukaryotic cells [20]. Therefore, these results collectively indicate that HI treatment not only induces oxidative DNA damage, but also induces DNA strand breaks damage.

It has been suggested that MTH1 is closely related to the survival of tumor cells [21–25]. For instance, MTH1 deficiency selectively increased non-cytotoxic oxidative DNA damage in lung cancer cells [26]. However, the role of MTH1 in AIT remains unclear. Importantly, here, we found that overexpression of MTH1 significantly reversed the HI-induced enhancement of inflammation, apoptosis, and DNA damage in mouse thyroid follicular epithelial cells. These results suggest that the enhanced inflammation, apoptosis, and DNA damage in AIT caused by HI treatment may be mediated, at least partially, through influencing the DNA repair capacity.

5. Conclusion

In conclusion, HI treatment induces inflammation, apoptosis, and DNA damage in AIT, at least in part, by inhibiting the DNA repair protein MTH1. Our findings provide a new perspective for elucidating the mechanism underlying the HI-induced AIT.

Declaration of Competing Interest

The authors declare no conflicts of interest.

Acknowledgements

Not applicable.

Funding

The research study was supported by the Health department of Zhejiang Province (2013KYA075) and the Zhejiang Provincial Natural Science Foundation of China (LY19H070004).

References

[1] N. Zhao, H. Zou, J. Qin, C. Fan, Y. Liu, S. Wang, Z. Shan, W. Teng, Y. Li, MicroRNA-326 contributes to autoimmune thyroiditis by targeting the Ets-1 protein, Endocrine 59 (2018) 120–129.
[2] G. Di Dalmazi, P. Chalan, P. Caturegli, MYMD-1, a Novel Immunometabolic Regulator, Ameliorates Autoimmune Thyroiditis via Suppression of Th1 Responses and TNF-alpha Release, J. Immunol. (Baltimore, Md. : 1950) (2019).
[3] S. Hu, M.P. Rayman, Multiple Nutritional Factors and the Risk of Hashimoto's Thyroiditis, Thyroid: Off. J. Am. Thyroid Assoc. 27 (2017) 597–610.
[4] I. Sachmechi, A. Khalid, S.I. Awan, Z.R. Malik, M. Sharifzadeh, Autoimmune Thyroiditis with Hypothyroidism Induced by Sugar Substitutes, Cureus 10 (2018) e3268.
[5] L.H. Duntas, The role of iodine and selenium in autoimmune thyroiditis, Hormone and metabolic research = Hormon- und Stoffwechselforschung = Hormones et metabolisme 47 (2015) 721–726.
[6] T. Giassa, I. Mamali, E. Gaki, G. Kaltsas, G. Kouraklis, K. Markou, T. Karatzas, Iodine intake and chronic autoimmune thyroiditis: a comparative study between coastal and mainland regions in Greece, Hormones (Athens, Greece) 17 (2018) 565–571.
[7] J. Duan, J. Kang, T. Deng, X. Yang, M. Chen, Exposure to DBP and High Iodine Aggravates Autoimmune Thyroid Disease Through Increasing the Levels of IL-17 and Thyroid-Binding Globulin in Wistar Rats, Toxicol. Sci: An Off. J. Soc. Toxicol. 163 (2018) 196–205.
[8] X. He, C. Xiong, A. Liu, W. Zhao, X. Xia, S. Peng, C. Li, M. Zhou, Y. Li, X. Shi, Z. Shan, W. Teng, Phagocytosis Deficiency of Macrophages in NOD.H-2(h4) Mice Accelerates the Severity of Iodine-Induced Autoimmune Thyroiditis, Biol. Trace Elem. Res. 184 (2018) 196–205.
[9] L.H. Duntas, The catalytic role of iodine excess in loss of homeostasis in autoimmune thyroiditis, Curr. Opin. Endocrinol. Diabetes Obes. 25 (2018) 347–352.
[10] H. Braley-Mullen, S. Yu, NOD.H-2h4 mice: an important and underutilized animal model of autoimmune thyroiditis and Sjogren's syndrome, Adv. Immunol. 126 (2015) 1–43.
[11] S. Gonzalez-Rojo, C. Fernandez-Diez, S.M. Guerra, V. Robles, M.P. Herraez, Differential gene susceptibility to sperm DNA damage: analysis of developmental key genes in trout, PLoS ONE 9 (2014) e114161.
[12] A.I. Elkady, R.A.E.H. Hussein, O.A. Abu-Zinadah, Effects of crude extracts from medicinal herbs Rhazya stricta and Zingiber officinale on growth and proliferation of human brain cancer cell line in vitro, BioMed Res. Int. 2014 (2014) 260210–260210.
[13] J. You, Z. Yue, S. Chen, Y. Chen, X. Lu, X. Zhang, P. Shen, J. Li, Q. Han, Z. Li, P. Liu, Receptor-interacting Protein 140 represses Sirtuin 3 to facilitate hypertrophy, mitochondrial dysfunction and energy metabolic dysfunction in cardiomyocytes, Acta Physiol. (Oxford, England) 220 (2017) 58–71.
[14] A. Saha, S. Mukherjee, A. Bhattacharjee, D. Sarkar, A. Chakraborty, A. Banerjee, A.K. Chandra, Excess iodine-induced lymphocytic impairment in adult rats, Toxicol. Mech. Methods 29 (2019) 110–118.
[15] S. Kawanishi, S. Ohnishi, N. Ma, Y. Hiraku, M. Murata, Crosstalk between DNA Damage and Inflammation in the Multiple Steps of Carcinogenesis, Int. J. Mol. Sci. 18 (2017).
[16] E. Markkanen, Not breathing is not an option: How to deal with oxidative DNA damage, DNA Repair 59 (2017) 82–105.
[17] Y. Kikuchi, T. Yasuhara, T. Agari, A. Kondo, S. Kuramoto, M. Kameda, T. Kadota, T. Baba, N. Tajiri, F. Wang, J.T. Tayra, H. Liang, Y. Miyoshi, C.V. Borlongan, I. Date, Urinary 8-OHdG elevations in a partial lesion rat model of Parkinson's disease correlate with behavioral symptoms and nigrostriatal dopaminergic depletion, J. Cell. Physiol. 226 (2011) 1390–1398.
[18] H. Gad, T. Koolmeister, A.S. Jemth, S. Eshtad, S.A. Jacques, C.E. Strom, L.M. Svensson, N. Schultz, T. Lundback, B.O. Einarsdottir, A. Saleh, C. Gokturk, P. Baranczewski, R. Svensson, R.P. Berntsson, R. Gustafsson, K. Stromberg, K. Sanjiv, M.C. Jacques-Cordonnier, M. Desroses, A.L. Gustavsson, R. Olofsson, F. Johansson, E.J. Homan, O. Loseva, L. Brautigam, L. Johansson, A. Hoglund, A. Hagenkort, T. Pham, M. Altun, F.Z. Gaugaz, S. Vikingsson, B. Evers, M. Henriksson, K.S. Vallin, O.A. Wallner, L.G. Hammarstrom, E. Wiita, I. Almlof, C. Kalderen, H. Axelsson, T. Djureinovic, J.C. Puigvert, M. Haggblad, F. Jeppsson, U. Martens, C. Lundin, B. Lundgren, I. Granelli, A.J. Jensen, P. Artursson, J.A. Nilsson, P. Stenmark, M. Scobie, U.W. Berglund, T. Helleday, MTH1 inhibition eradicates cancer by preventing sanitation of the dNTP pool, Nature 508 (2014) 215–221.
[19] S. Koketsu, T. Watanabe, H. Nagawa, Expression of DNA repair protein: MYH, NTH1, and MTH1 in colorectal cancer, Hepatogastroenterology 51 (2004) 638–642.
[20] A.R. Collins, The comet assay for DNA damage and repair: principles, applications, and limitations, Mol. Biotechnol. 26 (2004) 249–261.
[21] M. Pompsch, J. Vogel, F. Classen, P. Kranz, G. Iliakis, H. Riffkin, U. Brockmeier, E. Metzen, The presumed MTH1-inhibitor TH588 sensitizes colorectal carcinoma cells to ionizing radiation in hypoxia, BMC Cancer 18 (2018) 1190.
[22] X.L. Shi, Y. Li, L.M. Zhao, L.W. Su, G. Ding, Delivery of MTH1 inhibitor (TH287) and MDR1 siRNA via hyaluronic acid-based mesoporous silica nanoparticles for oral cancers treatment, Colloids Surf B Biointerfaces 173 (2019) 599–606.
[23] L.M. van der Waals, J. Laoukili, J.M.J. Jongen, D.A. Raats, I.H.M. Borel Rinkes, O. Kranenburg, Differential anti-tumour effects of MTH1 inhibitors in patient-derived 3D colorectal cancer cultures, Sci. Rep. 9 (2019) 819.
[24] Z. Versano, E. Shany, S. Freedman, L. Tuval-Kochen, M. Leitner, S. Paglin, A. Toren, M. Yalon, MutT homolog 1 counteracts the effect of anti-neoplastic treatments in adult and pediatric glioblastoma cells, Oncotarget 9 (2018) 27547–27563.
[25] J.Y. Wang, G.Z. Liu, J.S. Wilmott, T. La, Y.C. Feng, H. Yari, X.G. Yan, R.F. Thorne, R.A. Scolyer, X.D. Zhang, L. Jin, Skp2-mediated stabilization of MTH1 promotes survival of melanoma cells upon oxidative stress, Cancer Res. 77 (2017) 6226–6239.
[26] H.H.K. Abbas, K.M.H. Alhamoudi, M.D. Evans, G.D.D. Jones, S.S. Foster, MTH1 deficiency selectively increases non-cytotoxic oxidative DNA damage in lung cancer cells: more bad news than good? BMC cancer 18 (2018) 423.